Supplement of

Photoenhanced sulfates formation by the heterogeneous uptake of SO_2 on non-photoactive mineral dust

Chong Han*, Jiawei Ma, Wangjin Yang, Hongxing Yang

School of Metallurgy, Northeastern University, Shenyang, 110819, China

*Address correspondence to author: hanch@smm.neu.edu.cn

This file includes:

Figures S1-S11

Tables S1

SI References

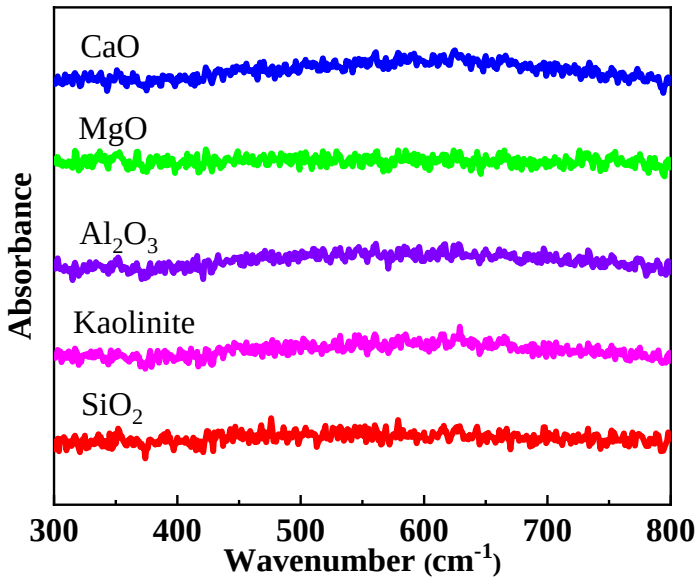

Figure S1. The UV-vis light absorption spectra of SiO_2, kaolinite, Al_2O_3, MgO and CaO.

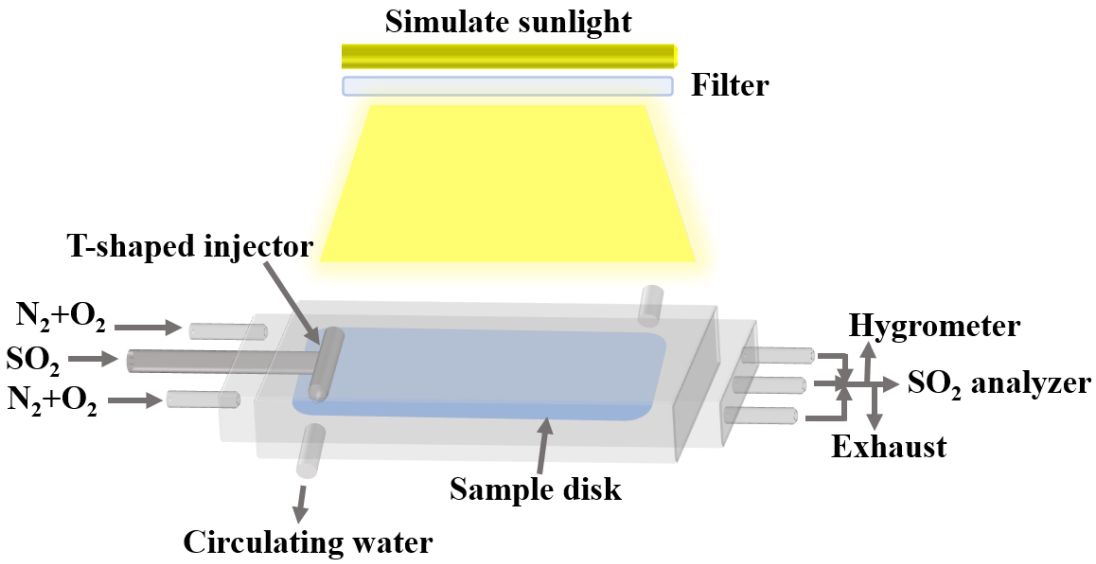

Figure S2. Diagram of the rectangular flow reactor.

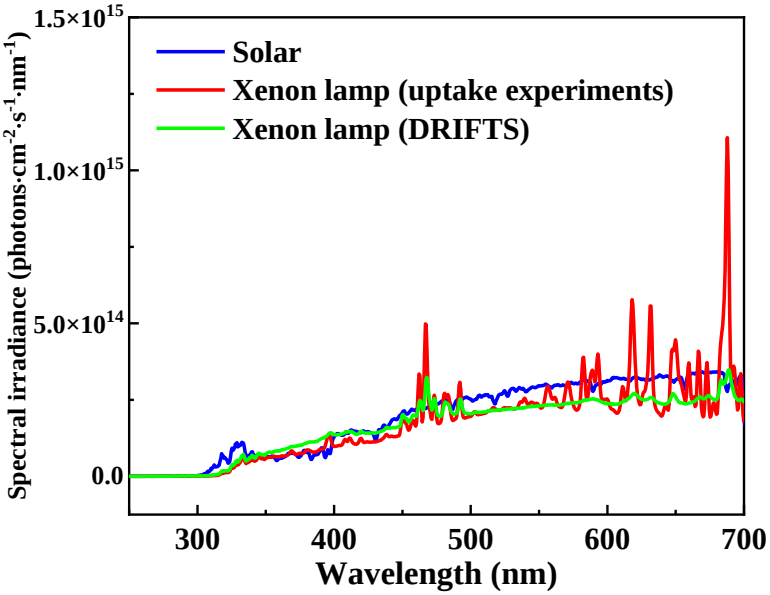

Figure S3. The spectral irradiance of the xenon lamp for SO_2 uptake and DRIFTS experiments and the solar for the 48° solar zenith clear sky at Shenyang (41.45N, 123.25E) on June 6th, 2022, at 12:00 local time.

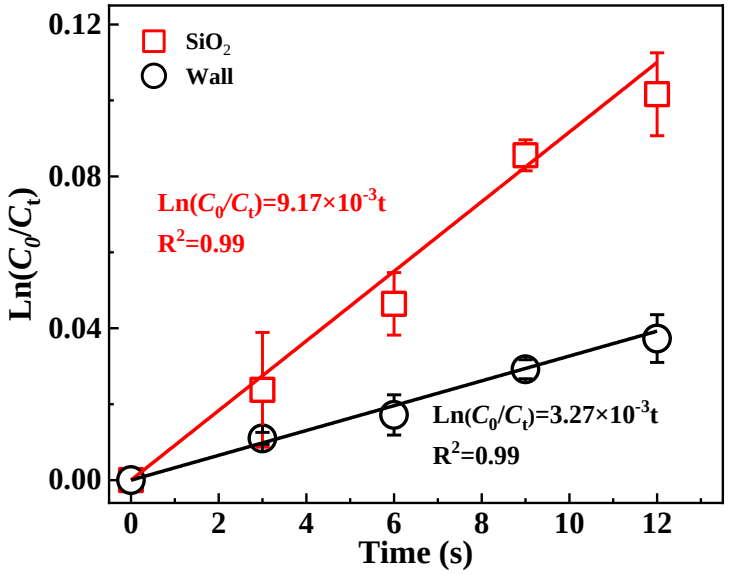

Figure S4. Determination of the linearity of ln(C_0/C_t) against the reaction time by varying the length of SiO_2 coating (red) and the blank reactor (black) contacting with SO_2. Reaction conditions: SiO_2 mass of 0.2 g, irradiation intensity of 250 W m^{-2}, temperature of 298 K, RH of 40% and O_2 content of 20%.

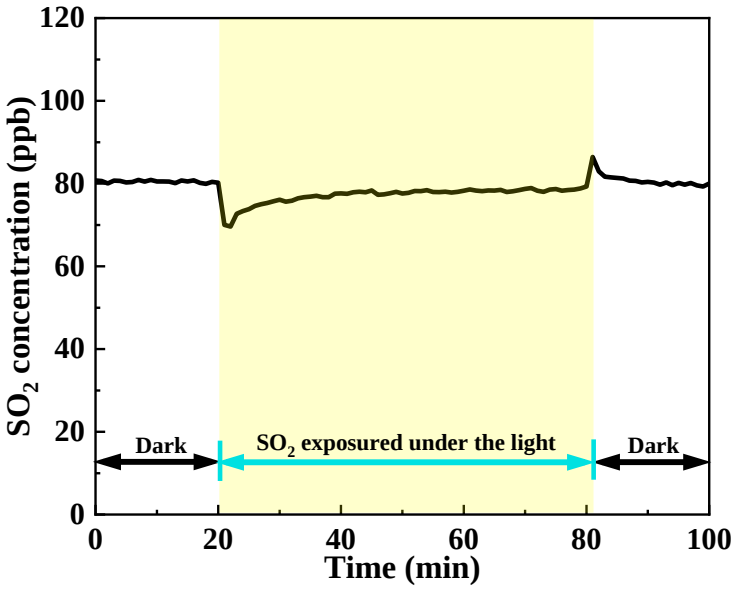

Figure S5. The temporal variation of SO_2 in blank experiments under irradiation. Reaction conditions: blank flow reactor, irradiation intensity of 250 W m^{-2}, RH of 40%, temperature of 298 K, and O_2 content of 20%.

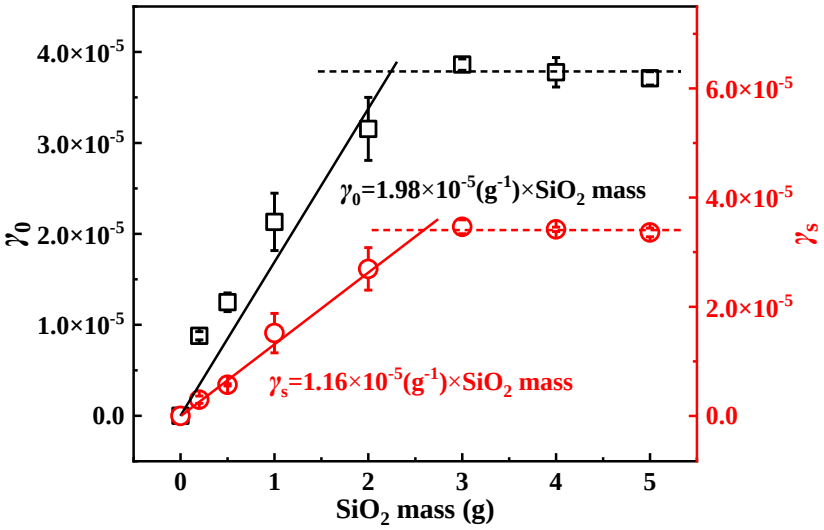

Figure S6. Initial uptake coefficients and steady-state uptake coefficients of SO_2 as a function of the SiO_2 mass.

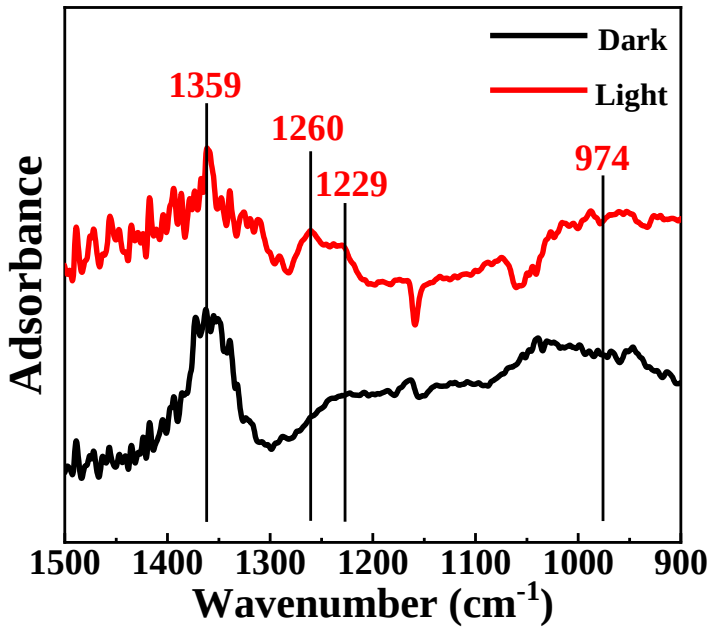

Figure S7. *In situ* DRIFTS spectra of SiO_2 in the range of 1500−900 cm^{-1} during the uptake process of SO_2 (2 ppm) for 600 min in the dark and under irradiation.

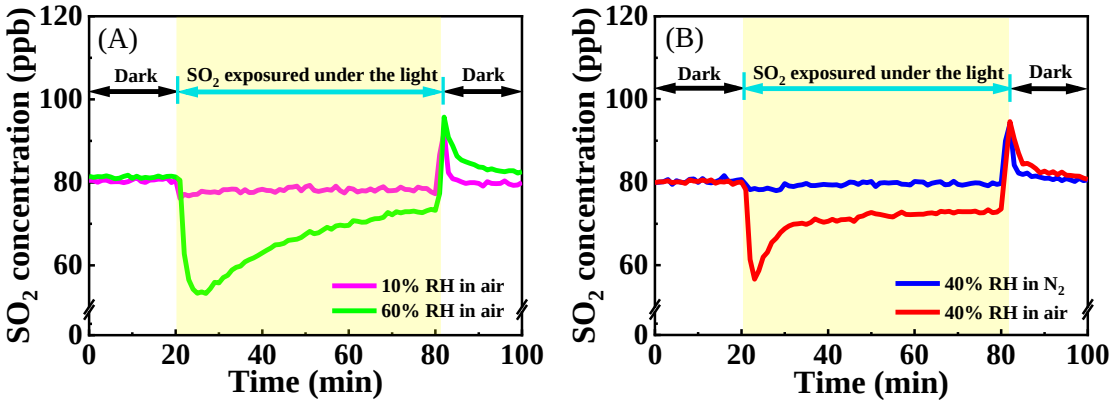

Figure S8. (A) Temporal variations of the SO_2 concentration on SiO_2 at different RHs. (B) Temporal variations of the SO_2 concentration on SiO_2 in N_2 and air. The background changes of the SO_2 concentration in the blank reactor have been deducted. Reaction conditions: SiO_2 mass of 0.2 g, irradiation intensity of 250 W m^{-2}, temperature of 298 K, O_2 content of 20% for (A) and RH of 40% for (B).

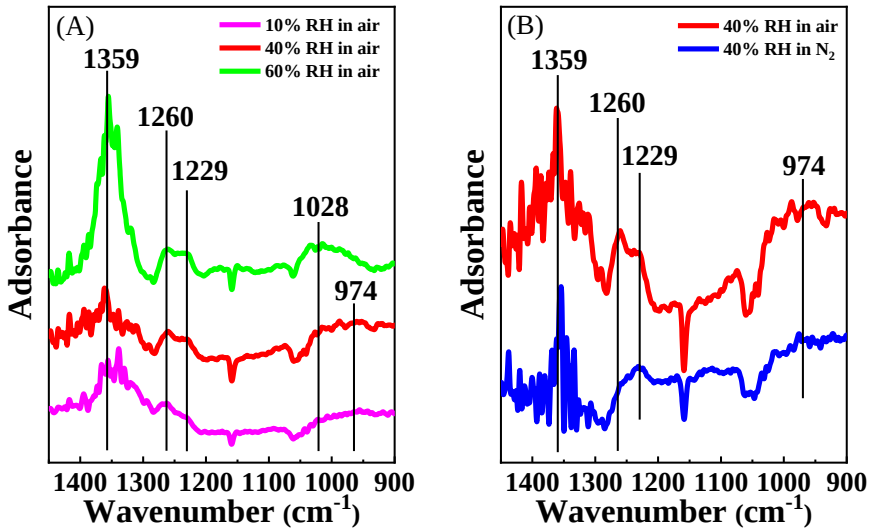

Figure S9. *In situ* DRIFTS spectra of SiO_2 during the uptake process of SO_2 (2 ppm) under different RHs (A) and O_2 contents (B).

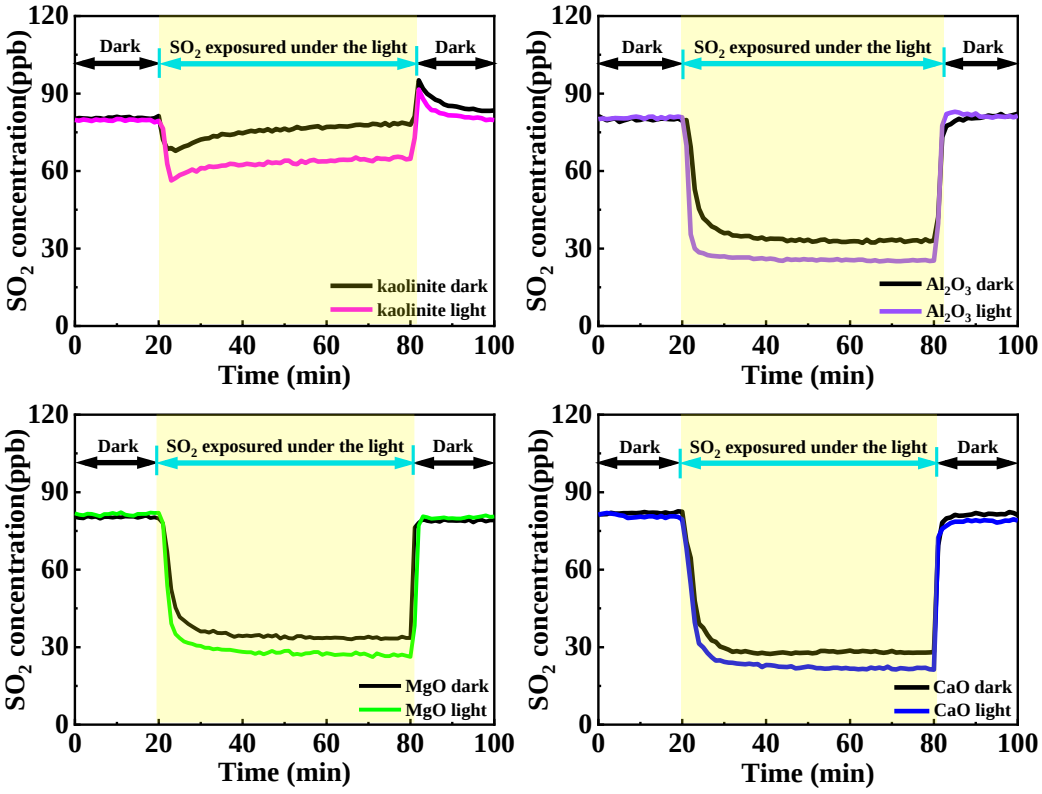

Figure S10. Temporal variations of the SO_2 concentration on kaolinite, Al_2O_3, MgO and CaO.

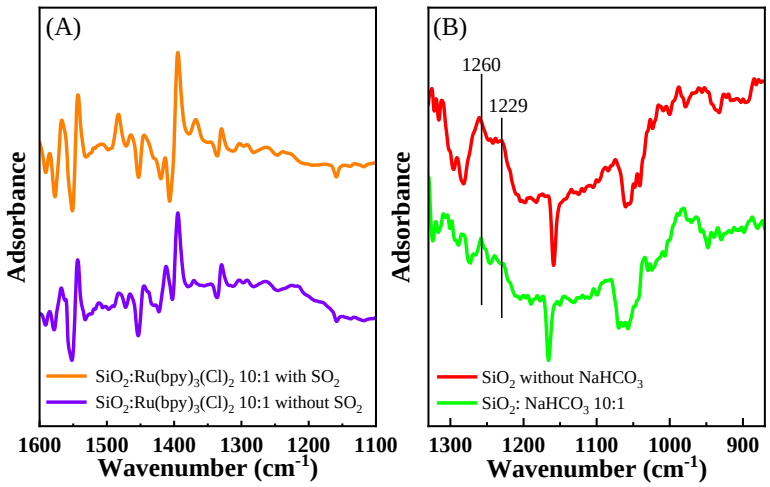

Figure S11. (A) *In situ* DRIFTS spectra on the surface of SiO_2 mixed with $Ru(bpy)_3(Cl)_2$ in the absence (purple line) and presence of SO_2 (yellow line) for 300 min. (B) *In situ* DRIFTS spectra during the uptake process of SO_2 (2 ppm) in the absence (red line) and presence of $NaHCO_3$ (green line) for 300 min.

Table S1. SO_2 uptake coefficients and sulfate formation rates in different pathways.

Pathways	Light sources	SO_2 uptake coefficients	Sulfate formation rates ($\mu g\ m^{-3}\ h^{-1}$)
•OH(Xue et al., 2016)	-	-	0.001–0.1
NO_2(Cheng et al., 2016)	-	-	0.01–10
H_2O_2(Liu et al., 2020a)	-	-	0.07–3.6
TMI(Ye et al., 2021)	-	2.56×10^{-10}	~0.001
nitrate(Gen et al., 2019)	UV	7.36×10^{-7}	0.001–1
black carbon(Zhang et al., 2022)	Xenon lamp	-	0.01–0.018
brown carbon(Liu et al., 2020b)	Xenon lamp	2×10^{-5}	0.19
$PM_{2.5}$(Zhang et al., 2020)	UV	4.82×10^{-7}	0.016
non-photoactive mineral dust	Xenon lamp	[a]2.22×10^{-6}	2.15

[a]This SO_2 uptake coefficient was calculated acconting for the mass fraction of SiO_2, Al_2O_3, MgO, and CaO in mineral dust, which was 60%, 12.5%, 4% and 6.5%, respectively.

Reference

Cheng, Y., Zheng, G., Wei, C., Mu, Q., Zheng, B., Wang, Z., Gao, M., Zhang, Q., He, K., Carmichael, G., Pöschl, U., and Su, H.: Reactive nitrogen chemistry in aerosol water as a source of sulfate during haze events in China, Sci. Adv., 2, 1601530-1601540, https://doi.org/10.1126/sciadv.1601530, 2016.

Gen, M., Zhang, R., Huang, D., Li, Y., and Chan, C.: Heterogeneous oxidation of SO_2 in sulfate production during nitrate photolysis at 300 nm: Effect of pH, relative humidity, irradiation intensity, and the presence of organic compounds, Environ. Sci. Technol., 53, 8757-8766, https://doi.org/10.1021/acs.est.9b01623, 2019.

Liu, T., Clegg, S., and Abbatt, J.: Fast oxidation of sulfur dioxide by hydrogen peroxide in deliquesced aerosol particles, Proc. Natl. Acad. Sci. U. S. A., 117, 1354-1359, https://doi.org/10.1073/pnas.1916401117, 2020a.

Liu, Y., Wang, T., Fang, X., Deng, Y., Cheng, H., Bacha, A. U., Nabi, I., and Zhang, L.: Brown carbon: An underlying driving force for rapid atmospheric sulfate formation and haze event, Sci. Total. Environ., 734, 139415-139424, https://doi.org/10.1016/j.scitotenv.2020.139415, 2020b.

Xue, J., Yuan, Z., Griffith, S. M., Yu, X., Lau, A. K., and Yu, J. Z.: Sulfate formation enhanced by a cocktail of high NO_X, SO_2, particulate matter, and droplet pH during haze-fog events in megacities in china: An observation-based modeling investigation, Environ. Sci. Technol., 50, 7325-7334, https://doi.org/10.1021/acs.est.6b00768, 2016.

Ye, C., Chen, H., Hoffmann, E. H., Mettke, P., Tilgner, A., He, L., Mutzel, A., Bruggemann, M., Poulain, L., Schaefer, T., Heinold, B., Ma, Z., Liu, P., Xue, C., Zhao, X., Zhang, C., Zhang, F., Sun, H., Li, Q., Wang, L., Yang, X., Wang, J., Liu, C., Xing, C., Mu, Y., Chen, J., and Herrmann, H.: Particle-phase photoreactions of HULIS and TMIs establish a strong source of H_2O_2 and particulate sulfate in the winter north china plain, Environ. Sci. Technol., 55, 7818-7830, https://doi.org/10.1021/acs.est.1c00561, 2021.

Zhang, P., Chen, T., Ma, Q., Chu, B., Wang, Y., Mu, Y., Yu, Y., and He, H.: Diesel soot photooxidation enhances the heterogeneous formation of H_2SO_4, Nat. Commun., 13, 5364-5372, https://doi.org/10.1038/s41467-022-33120-3, 2022.

Zhang, Y., Bao, F., Li, M., Xia, H., Huang, D., Chen, C., and Zhao, J.: Photoinduced uptake and oxidation of SO_2 on Beijing urban $PM_{2.5}$, Environ. Sci. Technol., 54, 14868-14876, https://doi.org/10.1021/acs.est.0c01532, 2020.